

The complementary subset of asymptotes is given by $\tan(\phi_n + \psi_n) = \infty$, or, developing the tangent and using (A2) and (A3)

$$G(u) = \left(\frac{\tan vh_1}{v} \right) \left(\frac{\tan vh_3}{v} \right) = \frac{1}{u^2}. \quad (\text{A6})$$

The left-hand member of (A6) is the product of two monotonous functions but is not monotonous. However, a careful examination of $G(u)$ shows that between 0 and the m th asymptote u'_m of $G(u)$, the number of solutions of (A6) is equal to m .

Now, the values of u'_m are analytic and given by

$$vh_1 = (2q+1) \frac{\pi}{2} \quad (\text{A7})$$

or

$$vh_3 = (2q'+1) \frac{\pi}{2}. \quad (\text{A8})$$

Finally, in an interval $(0, u'_m)$, we are able to determine the number m of non-analytic asymptotes of $F(u)$, thus to derive the total number $n = m + m'$ of asymptotes, m' being the number of analytic asymptotes given by (A5) between 0 and u'_m .

To compute the successive zeros of $F(u)$, we calculate $F(u)$ at a certain number P of equidistant points between 0 and u'_m . We detect the approximate positions of the zeros (when the sign of $F(u)$ goes from a negative to a positive value) and of the asymptotes (the opposite). The number n' of computed asymptotes compared to $n = m + m'$. If $n' < n$, the computation is started again, with $2P$ points, then $4P$ points, etc, as long as n' is not equal to n . So, we know that all the asymptotes have been detected, and it suffices to verify that a zero of $F(u)$ has well been found between two consecutive asymptotes to be sure that no zero has been forgotten until the last asymptote. A second step of the computation is to enhance the precision on the zeros by using the method of the secant, starting from the approximate values.

As regards the numerical implementation, this very effective systematic method appears to be necessary since the numerical exploitation has shown that $F(u)$ can have zeros and asymptotes very close to each other. Therefore, a rough search for the zeros often misses some of them, which is catastrophic for the final result.

REFERENCES

- [1] H. M. O'Bryan, J. Thomson, and J. K. Plourde, "A new BaO-TiO₂ compound with temperature stable high permittivity," *J. Amer. Ceram. Soc.*, vol. 57, pp. 450-453, Oct. 1974.
- [2] J. K. Plourde and Chung-Li Ren, "Application of dielectric resonators in microwave components," *IEEE Trans. Microwave Theory Tech.*, vol. MTT-29, pp. 754-770, Aug. 1981.
- [3] M. Gastine, L. Courtois, and J. L. Dormann, "Electromagnetic resonances of free dielectric spheres," *IEEE Trans. Microwave Theory Tech.*, vol. MTT-15, p. 694, Dec. 1967.
- [4] B. W. Hakki and P. D. Coleman, "A dielectric resonator method of measuring inductive capacities in the millimeter range," *IRE Trans. Microwave Theory Tech.*, vol. MTT-8, pp. 402-410, July 1960.
- [5] W. E. Courtney, "Analysis and evaluation of a method of measuring the complex permittivity," *IEEE Trans. Microwave Theory Tech.*, vol. MTT-18, p. 476, Aug. 1970.
- [6] P. Guillou and Y. Garrault, "Correction to accurate resonant frequencies of dielectric resonators," *IEEE Trans. Microwave Theory Tech.*, vol. MTT-28, p. 434, Apr. 1980.
- [7] M. Dydyk, "Dielectric resonators add Q to MIC filters," *Microwaves*, vol. 16, p. 150, Dec. 1977.
- [8] M. Dydyk, "Apply high Q resonators to mm-wave microstrips," *Microwaves*, vol. 19, no. 13, p. 62, Dec. 1980.
- [9] R. R. Bonetti and A. E. Atia, "Design of cylindrical dielectric resonators in inhomogeneous media," *IEEE Trans. Microwave Theory Tech.*, vol. MTT-29, pp. 323-326.
- [10] M. Jaworski and M. W. Pospiszalski, "An accurate solution to the cylindrical dielectric resonator problem," *IEEE Trans. Microwave Theory Tech.*, vol. MTT-27, pp. 639-643, July 1979.

- [11] T. Itoh and R. Rudokas, "New method for computing the resonant frequency of dielectric resonators," *IEEE Trans. Microwave Theory Tech.*, vol. MTT-25, pp. 52-56, Jan. 1977.
- [12] R. Courant and D. Hilbert, *Methods of Mathematical Physics*. New York: Interscience, 1965, p. 360.

Moment-Method Solutions and SAR Calculations for Inhomogeneous Models of Man with Large Number of Cells

JOHN F. DEFORD, OM P. GANDHI, FELLOW, IEEE, AND MARK J. HAGMANN, MEMBER, IEEE

Abstract — This paper describes an iterative band approximation method (BAM) that is useful for solution of large matrix equations where the elements of the matrix decrease in magnitude with increasing distance from the diagonal. The method involves the inversion of a band about the diagonal which is used to obtain a first estimate of the solution. This estimate, along with the remaining elements in the matrix above and below the band, is used to iterate to the final solution. Due to the substantial reduction in the size of the matrix which is actually inverted, the method has been applied to the solution of full complex matrix equations involving up to 1698 unknowns. BAM is used to obtain distributions of EM energy absorption for man models with 180-1132 cells.

I. INTRODUCTION

To understand the biological effects of electromagnetic fields, it is necessary to quantify the whole-body absorption and its distribution for the various irradiation conditions. Moment-method solutions with inhomogeneous man models have been used to obtain the distributions of time-rates of absorbed energy (specific absorption rates (SAR's)) for free-space irradiation [1]-[3], for a human in contact with and slightly removed from a ground plane and in the presence of metallic corner reflectors [4]. Combined with the plane-wave-spectrum approach to prescribe the incident fields, moment-method solutions have also been used to obtain SAR distributions for leakage-type (uncoupled) near-field exposure conditions such as those from RF sealers, etc. [5]. In fact, in spite of the claims made for other numerical approaches such as finite-element methods, etc., the moment-method is the only successful procedure used at the present time to obtain SAR distributions for inhomogeneous models of biological bodies.

Most of our work has used a block model of man using 180 cubical cells of various sizes arranged for a best fit of the contour on diagrams of the 50th percentile standard man [3]. With considerably larger computation times, we have also described solutions in which a total of 340 cells were used to provide a finer detail of energy deposition in the head and neck allowing us to pinpoint the frequency region for head resonance [6]. The procedures used in the past have required the use of full complex matrices $3N \times 3N$ in dimension for a model with N cells. Effi-

Manuscript received November 15, 1982; revised April 18, 1983. This work was supported by NIEHS under grant ES02304.

J. DeFord and O. Gandhi are with the Department of Electrical Engineering, University of Utah, Salt Lake City, UT 84112.

M. Hagmann is with the National Institutes of Health, Bethesda, MD.

cient procedures are consequently needed for inversion of such large matrices so that a larger number of cells may be used for a more accurate calculation of energy distribution, without a substantial increase in the computation cost.

This paper describes an efficient algorithm called the band-approximation method (BAM) for inversion of large matrices and its use for man models with large number of cells up to 1132. This method was originally suggested by Ferguson, *et al.* [11] but was implemented only for relatively small problems involving 100 unknowns or less.

II. THE BAND-APPROXIMATION METHOD

For this method to succeed it is essential that the matrix elements show a band-like structure around the diagonal. Due to the properties of the Green's function, the matrix \vec{A} in the moment-method equation [1]–[3] can be made to have a rapid decrease in the magnitude of the elements with increasing distance from the diagonal by a properly ordered numbering of the cells in the model.

The moment-method matrix equation to be solved has the form

$$\vec{A} \cdot \vec{E} = \vec{E}' \quad (1)$$

where the vectors \vec{E} and \vec{E}' are the values of total electric field and incident electric field within the cells of the model and \vec{A} is the matrix involving the derivatives of the Green's function and the complex dielectric properties of the individual cells.

Let \vec{B} be a banded section about the diagonal of matrix \vec{A} . Also let $\vec{C} = \vec{A} - \vec{B}$ be the rest of the matrix \vec{A} . We can rewrite (1) as

$$\vec{B} \cdot \vec{E} + \vec{C} \cdot \vec{E} = \vec{E}' \quad (2)$$

or

$$\vec{E} = (\vec{B}^{-1} \cdot \vec{E}') - (\vec{B}^{-1} \cdot \vec{C}) \cdot \vec{E}. \quad (3)$$

Iterations for BAM are defined by

$$\vec{E}_{j+1} = \alpha(\vec{B}^{-1} \cdot \vec{E}') + [(1 - \alpha)\vec{I} - \alpha(\vec{B}^{-1} \cdot \vec{C})] \cdot \vec{E}_j \quad (4)$$

where \vec{I} is the unit matrix and α is the relaxation factor.

Since matrix \vec{A} is diagonally dominant, the LU decomposition of \vec{B} does not require pivoting and so preserves bandwidth. Hence, in implementing BAM, the banded portion \vec{B} may be overwritten with its LU factors. This is increasingly important as the matrix becomes larger since it dramatically reduces the computer memory requirements.

Let \vec{e}_j define the error $\vec{E}_j - \vec{E}$ of the j th iteration from the exact solution \vec{E} , then \vec{e}_{j+1} can be written as

$$\vec{e}_{j+1} = [(1 - \alpha)\vec{I} - \alpha(\vec{B}^{-1} \cdot \vec{C})] \cdot \vec{e}_j. \quad (5)$$

For $\alpha \leq 1$, the convergence of the iterations is assured if all eigenvalues of $(\vec{B}^{-1} \cdot \vec{C})$ have magnitudes less than unity. The rapid decrease in magnitude of the elements with increasing distance from the diagonal guarantees that this condition is satisfied, and hence convergence will invariably occur for a sufficiently large value of bandwidth.

III. TESTING WITH A 180-CELL MODEL OF MAN

A series of tests of BAM has been made using the 180-cell block model of man [3]. Since one plane of symmetry was used in the model, the matrix was 270×270 in dimension. Bounds on the limiting bandwidth for convergence are shown in Fig. 1. Note

¹LU decomposition is the factorization of a matrix into a lower triangular matrix and an upper triangular matrix [7].

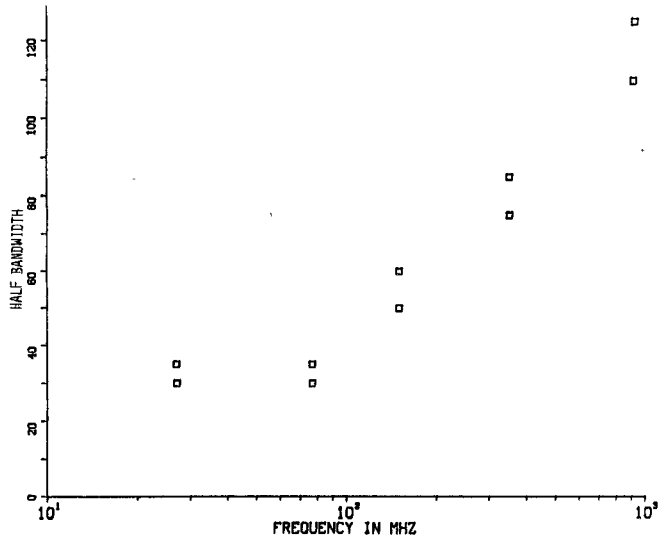


Fig. 1. Bandwidth for convergence of iterations with a 180-cell block model of man. No relaxation was used.

that the limiting bandwidth is an increasing function of frequency. This is attributed to an observed decrease in rolloff of matrix element magnitudes with distance from the diagonal on account of increased dominance of radiation ($1/R$) terms at higher frequencies. No relaxation was required for solution of the 180-cell man model, but we found that solution of man models containing more than approximately 400 cells required underrelaxation. Total computer time for the solutions was about $1/3$ that of a noniterative solution at 915 MHz, and considerably less at lower frequencies due to decreased bandwidth.

IV. APPLICATIONS TO MAN MODELS WITH LARGER NUMBER OF CELLS

In addition to finer discretization of the biological bodies or parts thereof, the models with larger numbers of cells also permit a more accurate geometric representation of these bodies. The BAM has been used to obtain SAR distributions for the following man models.

1) An 1132-cell homogeneous model of man with dielectric properties corresponding to $2/3$ muscle [8]. For this model, each of the cubical blocks in our 180-cell model [3] is divided into eight cubical blocks. Some of the cells were then deleted or put in slightly different locations in order to improve the physical conformity of the model to a human body.

2) A 626-cell inhomogeneous model of man shown in Fig. 2. This model is similar to the 1132-cell model except that somewhat coarser cells are used in the torso and the arms. The volume-averaged complex permittivities for the individual cells are obtained from the anatomical data [9] on the composition of tissues (fat, muscle, skin, bone, etc.) in the respective regions and the known frequency-dependent permittivities [8] for the various constituents.

3) Intermediate models, where individual regions of the body were finely discretized leaving the rest of the body discretized as in the 180-cell model [3].

Pulse-function basis and delta functions for testing were used in applying the method of moments for solution of the electric-field integral equation. Since the solutions were obtained with a relatively small main frame computer (Digital Systems DEC-20), it was necessary to use only a small fraction of the center band in

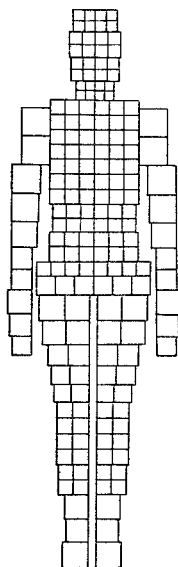


Fig. 2. Front view of a 626-cell model of man.

TABLE I
SOME TYPICAL COMPUTATION TIMES ON THE DEC-20 FOR THE
VARIOUS MAN MODELS

Number of Cells	Frequency MHz	Half-Bandwidth	Number of Iterations	Computation Time h, min
180	27.12	50	20	0, 5
180	350.00	100	20	0, 7
340	27.12	100	20	0, 22
340	350.00	180	20	0, 33
580	27.12	250	30	1, 50
626	27.12	250	15	1, 21
626	77.00	250	38	2, 31
760	27.12	300	40	5, 9
1132	27.12	350	40	11, 36

"core" memory at any one time. Substantial time was therefore spent in swapping data back and forth from the disk.

A representative set of computation times for the various models is given in Table I. It is recognized that use of larger computers will allow a larger fraction of the data in the memory with a drastic reduction in the computation time. Almost three-fourths of the computer time necessary for the 1132-cell solution was expended in data acquisition from the disk.

V. RESULTS

The highlights of the SAR's calculated for the various models are given in Table II. Some of the salient features of the results may be summarized as follows.

1) The calculated values of the whole-body-averaged SAR increases with the number of cells that are used. This result is ascribed to the fact that an insufficient number of cells have been used to represent the actual field variations within the body. A similar effect was previously observed [10] for calculations of absorbed energy by a cubical body of saline. Asymptotically converging solutions were obtained with reasonable estimates obtained for cell sizes Δ such that $\Delta/\lambda_e < 0.1$ (λ_e is the wavelength in the material). Since such small cell sizes will imply man

TABLE II
WHOLE BODY AVERAGE AND NORMALIZED REGIONAL SAR'S FOR
THE VARIOUS MAN MODELS

	Homogeneous Models (27.12 MHz)			Inhomogeneous Models (27.12 MHz)	
	180 Cell	760* Cell	1132 Cell	180 Cell	626 Cell
Whole body Average SAR	.0105	.0139	.0161	.0134	.0207
Normalized Regional SARs = $\frac{\text{Regional SAR}}{\text{Whole Body SAR}}$					
Head	.54	.79	.69	.65	.35
Neck	1.68	2.94	2.56	1.53	1.68
Upper Arm	.11	.07	.05	.12	.06
Lower Arm	.14	.10	.08	.19	.11
Upper Torso	.47	.76	.66	.47	.43
Mid Torso	.58	.89	.79	.43	.44
Lower Torso	.70	.68	.79	.66	.71
Thigh	1.75	1.48	1.51	1.54	2.58
Calf	3.44	2.78	2.85	3.30	3.38

Note: This model was not evenly subdivided. The cells in and above the mid-torso region were substantially smaller than those used in the lower torso and in the legs.

models with 10^4 or more cells, they are obviously unsolvable with the moment-method approach that has been used to date.

2) As expected, the use of a larger number of cells helps to define the "hot spots" somewhat more sharply. Larger normalized SAR's are, for example, obtained for the neck region for models with a larger number of cells.

3) No trends can be delineated for the results of model with finer discretization for parts of the body. The normalized regional SAR's depend upon how much of the body was subdivided and the frequency of the incident field.

VI. CONCLUSIONS

A fundamental limitation of the moment-method is that inversion of full or nearly-full matrices is involved. Only a limited number of cells can, therefore, be used if the computation time is to be kept within affordable limits. The method does allow the use of realistic inhomogeneous models and is the only method available at the present time for calculations of SAR distributions. The development of the BAM outlined in this paper has allowed us to go up to 626- to 1132-cell models—a number unthinkable in the past. This has also highlighted the need for still finer discretization (smaller cells sizes $\Delta/\lambda_e < 0.1$), which is clearly impractical with any size computer presently available if the moment-method approach using pulse-function-basis is to be used. It should be mentioned here that the computation time goes up roughly as N^3 . The use of more complicated basis functions may reduce the number of cells necessary for the convergence of the solution, but, on the other hand, may also add to the computation time because of the complexity of the calculations. Development of numerically efficient procedures such as FFT, with computation times proportional to $N \log_2(N)$ per iteration, may allow use of 10^4 – 10^5 inhomogeneous cells permitting thereby a detailed modeling of the crucial regions of the body such as the eyes, the gonads, etc. Some pilot studies recently completed in our laboratory have demonstrated the feasibility of this approach.

REFERENCES

- [1] D. E. Livesay and K. M. Chen, "Electromagnetic fields induced inside arbitrary shaped biological bodies," *IEEE Trans. Microwave Theory Tech.*, vol. MTT-22, pp. 1273-1280, 1974.
- [2] K. M. Chen and B. S. Guru, "Internal EM field and absorbed power density in human torsos induced by 1-500 MHz EM waves," *IEEE Trans. Microwave Theory Tech.*, vol. MTT-25, pp. 746-756, 1977.
- [3] M. J. Hagmann, O. P. Gandhi, and C. H. Durney, "Numerical calculation of electromagnetic energy deposition for a realistic model of man," *IEEE Trans. Microwave Theory Tech.*, vol. MTT-27, pp. 804-809, 1979.
- [4] M. J. Hagmann and O. P. Gandhi, "Numerical calculation of electromagnetic energy deposition in man with ground and reflector effects," *Radio Sci.*, vol. 14, No. 6(5), pp. 23-29, 1979.
- [5] I. Chatterjee, M. J. Hagmann, and O. P. Gandhi, "Electromagnetic energy deposition in an inhomogeneous block model for near-field irradiation conditions," *IEEE Trans. Microwave Theory Tech.*, vol. MTT-28, pp. 1452-1459, 1980.
- [6] M. J. Hagmann, O. P. Gandhi, J. A. D'Andrea, and I. Chatterjee, "Head resonance: Numerical solutions and experiment results," *IEEE Trans. Microwave Theory Tech.*, vol. MTT-27, pp. 809-813, 1979.
- [7] A. Ralston and P. Rabinowitz, *A First Course in Numerical Analysis*, 2nd ed. New York: McGraw-Hill, 1975.
- [8] C. C. Johnson and A. W. Cory, "Nonionizing electromagnetic wave effects in biological materials and systems," *Proc. IEEE*, vol. 60, pp. 692-718, 1972.
- [9] D. J. Morton, *Manual of Human Cross-Section Anatomy*. Baltimore: Williams and Williams, 1944.
- [10] M. J. Hagmann, "Numerical studies of absorption of electromagnetic energy by man," *Ph.D. Dissertation*, Univ. of Utah, 1978.
- [11] T. R. Ferguson, T. H. Lehman, and R. J. Balestri, "Efficient solution of large moment problems: Theory and small problem results," *IEEE Trans. Antennas Propagat.*, vol. AP-24, pp. 230-235, 1976.

Letters

Comments on "Capabilities of Multi-Applicator Systems for Focused Hyperthermia"

PAUL F. TURNER

In the above paper¹, the author has incorrectly assumed that aperture size must be limited to a lateral dimension of not less than one wavelength in fat tissue in order to prevent excessive heating of superficial fat. The reference cited to support this conclusion [1] did not make such a generalization, but rather provided an example which implied this restriction at a particular frequency and with a certain aperture size. In actuality, however, focussed co-phased applicators are useful across a much broader range than Knoechel has suggested.

The work to which he has referred stems in turn from that of Guy and Lehmann [2]; this material indicates that an optimum frequency exists at which a single aperture produces minimum surface fat heating and maximal penetration depth through a fat/muscle boundary. Guy's study shows that only small changes in fat heating at lower frequencies occur through near-field effects.

The use of a dielectric (i.e., water-filled) bolus was alluded to by Knoechel, but he mentioned nothing of the effects of this device. In fact, such a bolus displaces the aperture near fields

from the tissue surface and at the same time acts as a dielectric waveguide to maintain energy confinement within the bolus. Fat heating can therefore be reduced at lower frequencies and with smaller apertures. The primary advantage of using lower frequencies in a co-phase applicator array is that this produces a larger central hot zone because of the longer wavelengths used.

A rather dramatic example of the use of synchronously arrayed radiators is the Annular Phased Array (APA), developed at BSD Medical Corporation, which is composed of 16 apertures surrounding the patient in an annular fashion. I first reported on this device and its test results in June of 1980 [3]; these initial tests demonstrated that a large central heating zone was created in muscle phantom models of the human trunk and in large pigs. No selective fat heating has been observed in subsequent animal experiments or in any of the more than 430 patient treatments to date.

A water bolus is placed between the apertures of the APA and the tissue in order to reduce near-field effects by lowering the medium impedance at the aperture and displacing the tissue from the near fields. This allows broad-band operation of the Annular Phased Array at frequencies of 50-110 MHz. Each of the 16 apertures of this device has a minimal size of 23 cm, which is one-eighth of a wavelength in fat at 50 MHz. The wavelength in muscle at 50 MHz is 47 cm [1]; thus, the central co-phase reinforcement zone is on the order of 24 cm wide.

Knoechel, however, in his article, did not clearly state the necessity for aligning the electric fields of co-phased apertures in

Manuscript received April 4, 1983.

The author is with BSD Medical Corporation, University of Utah Research Park, 420 Chipeta Way, Salt Lake City, UT 84108.

¹R. Knoechel, *IEEE Trans. Microwave Theory Tech.*, vol. MTT-30, Jan 1983.